

Journal of Mechanics of Materials and Structures

**DYNAMIC BEHAVIOR OF MAGNETOSTRICTIVE/PIEZOELECTRIC LAMINATE
CYLINDRICAL SHELLS DUE TO ELECTROMAGNETIC FORCE**

B. Biju, N. Ganesan and K. Shankar

Volume 6, No. 6

July–August 2011

DYNAMIC BEHAVIOR OF MAGNETOSTRICTIVE/PIEZOELECTRIC LAMINATE CYLINDRICAL SHELLS DUE TO ELECTROMAGNETIC FORCE

B. BIJU, N. GANESAN AND K. SHANKAR

The effect of electromagnetic force on the dynamic response of magnetostrictive/piezoelectric laminate cylindrical shells is addressed using a semianalytical finite element method. The electric field is represented using electric scalar potential and the magnetic field by magnetic vector potentials. The electric field acting on the charged particles of a moving conductor is derived from the Lorentz force. The mechanical force generated by the interaction of the derived current density with the magnetic field is accounted for in the successive load steps using an iterative solution technique. The Terfenol-D/PZT configuration of the laminate is analyzed for the first circumferential harmonics of the shell structure with a clamped-free boundary condition. The effect of electromagnetic force on the dynamic response is marginal at normal operating conditions but numerical studies suggest that the magnetoelectric effect is significantly influenced by a small increase in magnetic potential at increased velocities of the shell.

1. Introduction

Magnetostrictive/piezoelectric laminates have attracted attention for their magnetoelectric effects, originating from the electroelastic and magnetoelastic couplings inherent in the material. The composite consists of a piezoelectric phase, showing a coupling between the mechanical and electric fields, and a piezomagnetic phase, showing a coupling between the mechanical and magnetic fields. In addition, a magnetoelectric coupling effect, which is absent in the constituent phases, is exhibited by this class of materials. This unique feature allows magnetic control of electric polarization, electric control of magnetization, and control of electric and magnetic fields with mechanical stress, which make the material suitable for a wide range of applications such as magnetic field probes, medical ultrasound imaging, sensors, actuators, and so on.

The magnetoelectric properties of laminate composites of magnetostrictive/piezoelectric materials were investigated in [Ryu et al. 2001]. In [Sunar et al. 2002] the finite element modeling of a fully coupled thermopiezomagnetic medium using a thermodynamic potential was presented. A magnetic vector potential is needed to derive the elemental matrices using the above formulation. An analytical solution for the transient response of a magneto-electroelastic hollow cylinder was presented in [Hou and Leung 2004], where a plain strain condition with axisymmetric loading was used so that radial displacement only was considered to derive the solution. In [Dai and Wang 2006] an analytical solution was presented for the transient response of a magneto-electroelastic hollow cylinder placed in an axial magnetic field subjected to thermal shock, mechanical load, and transient electric excitation. The finite element formulation of MEE cylindrical shells using the magnetic vector potential in cylindrical coordinates was done in [Biju et al. 2010]. In [Shindo et al. 2010] the nonlinear electromagnetomechanical

Keywords: magnetostrictive/piezoelectric, magnetoelectric, electromagnetic force, finite element.

behavior of a magnetostrictive/piezoelectric laminate under a magnetic field was studied both numerically and experimentally.

The effect of electromagnetic force on the dynamic response of magnetostrictive/piezoelectric laminate cylindrical shells is addressed using a semianalytical finite element method in this paper. Dynamic loading will generate time-changing electric and magnetic fields in multifunctional smart materials. The electric field is represented using the electric scalar potential and modeling of the magnetic field is done using the magnetic vector potential in cylindrical coordinates. The current density acting on the charged particles of a moving conductor is evaluated using Ohm's law. The mechanical force generated by the interaction of the derived current density with the magnetic field is calculated using the Lorentz force equation and accounted for in the successive load steps using an iterative solution technique. Magnetostrictive Terfenol-D ($\text{Tb}_{0.3}\text{Dy}_{0.7}\text{Fe}_2$) and piezoelectric PZT ($\text{Pb}(\text{Zr},\text{Ti})\text{O}_3$) layers are used for modeling the axisymmetric cylindrical shell.

2. Theoretical formulation

2.1. Constitutive equations. The constitutive equations for the magnetostrictive/piezoelectric laminate in a cylindrical coordinate system (r, θ, z) relating stress σ_j , electric displacement D_l , and magnetic field intensity H_l to strain S_k , electric field E_m , and magnetic flux density B_m , exhibiting linear coupling between magnetic, electric, and elastic fields, can be written as (see [Shindo et al. 2010])

$$\sigma_j = C_{jk}S_k - e_{jm}E_m, \quad D_l = e_{lj}S_k - \epsilon_{lm}E_m, \quad (1)$$

for piezoelectric behavior and

$$\sigma_j = C_{jk}S_k - d_{jm}B_m, \quad H_l = -d_{lj}S_k - \mu_{lm}^{-1}B_m, \quad (2)$$

for magnetostrictive behavior. C_{jk} , ϵ_{lm} , and μ_{lm} are elastic, dielectric, and magnetic permeability coefficients, respectively, and e_{jl} and d_{jl} are the piezoelectric and piezomagnetic material coefficients ($d_{jl} = q_{jl}\mu_{lm}^{-1}$). Here $j, k = 1, \dots, 6$ and $l, m = 1, \dots, 3$.

2.2. Finite element modeling of electric and magnetic fields. The mechanical displacements, electric scalar potential, and magnetic vector potentials are expressed using Fourier series in the circumferential direction:

$$u_r = \sum u_r^n \cos n\theta, \quad u_\theta = \sum u_\theta^n \sin n\theta, \quad u_z = \sum u_z^n \cos n\theta, \quad \phi = \sum \phi^n \cos n\theta, \quad (3a)$$

$$A_r = \sum A_r^n \cos n\theta, \quad A_\theta = \sum A_\theta^n \sin n\theta, \quad A_z = \sum A_z^n \cos n\theta, \quad (3b)$$

where u_r , u_θ , and u_z are the radial, circumferential, and axial displacements, ϕ is the electric scalar potential, and A_r , A_θ , and A_z are the radial, circumferential, and axial components of the magnetic vector potential as nodal variables, respectively. Superscript n denotes the symmetric components of the primary variables: thus u_r^n , u_θ^n , u_z^n , ϕ^n , A_r^n , A_θ^n , and A_z^n .

The displacements $\{u\} = \{u_r, u_\theta, u_z\}^T$, electric potential (ϕ), and magnetic potential $\{A\} = \{A_r, A_\theta, A_z\}^T$ within the element can be expressed in terms of suitable shape functions:

$$\{u\} = [N_u]\{u^e\}, \quad \phi = [N_\phi]\{\phi^e\}, \quad \{A\} = [N_A]\{A^e\}. \quad (4)$$

The strains can be related to the nodal degree of freedom by the following expression:

$$\{S\} = [Bu]\{u^e\}, \tag{5}$$

where $[B_u]$, the strain displacement matrix, can be written as

$$[B_u] = \begin{bmatrix} \frac{\partial N_1}{\partial r} & 0 & 0 & \dots \\ \frac{N_1}{r} & \frac{nN_1}{r} & 0 & \dots \\ 0 & 0 & \frac{\partial N_1}{\partial z} & \dots \\ 0 & \frac{\partial N_1}{\partial z} & -\frac{nN_1}{r} & \dots \\ \frac{\partial N_1}{\partial z} & 0 & \frac{\partial N_1}{\partial r} & \dots \\ -\frac{nN_1}{r} & \frac{\partial N_1}{\partial r} & -\frac{N_1}{r} & 0 & \dots \end{bmatrix}. \tag{6}$$

Using the Maxwell’s relation, the electric field vector can be expressed as

$$\begin{Bmatrix} E_r \\ E_\theta \\ E_z \end{Bmatrix} = \begin{Bmatrix} -\frac{\partial \phi}{\partial r} \\ -\frac{1}{r} \frac{\partial \phi}{\partial \theta} \\ -\frac{\partial \phi}{\partial z} \end{Bmatrix} - \begin{Bmatrix} \dot{A}_r \\ \dot{A}_\theta \\ \dot{A}_z \end{Bmatrix}, \quad \{E\} = -[\nabla N_\phi]\{\phi^e\} - [N_A]\{\dot{A}_e\} = [B_\phi]\{\phi^e\} - [N_A]\{\dot{A}_e\}. \tag{7}$$

The derivative of the shape function matrix $[B_\phi]$ matrix is written as

$$[B_\phi] = \begin{bmatrix} -\frac{\partial N_1}{\partial r} & -\frac{\partial N_2}{\partial r} & -\frac{\partial N_3}{\partial r} & -\frac{\partial N_4}{\partial r} \\ \frac{nN_1}{r} & \frac{nN_2}{r} & \frac{nN_3}{r} & \frac{nN_4}{r} \\ -\frac{\partial N_1}{\partial z} & -\frac{\partial N_2}{\partial z} & -\frac{\partial N_3}{\partial z} & -\frac{\partial N_4}{\partial z} \end{bmatrix}. \tag{8}$$

Recalling Maxwell’s relations,

$$B = \nabla \times A, \quad \nabla \times H = J_0 + \frac{\partial D}{\partial t}, \tag{9}$$

where J_0 is the current supplied by an external source and $\partial D/\partial t$ is the displacement current. When dynamic mechanical loading is present, including the effect of the motion of the conductor, Ohm’s law can be written as

$$J = \sigma \left\{ E + \frac{\partial u}{\partial t} \times B \right\} + J_0, \tag{10}$$

where J is the total current density and σ is the electrical conductivity of the material.

In cylindrical coordinates

$$\nabla \times A = \hat{r} \left(\frac{1}{r} \frac{\partial A_z}{\partial \theta} - \frac{\partial A_\theta}{\partial z} \right) + \hat{\theta} \left(\frac{1}{r} \frac{\partial A_r}{\partial z} - \frac{\partial A_z}{\partial r} \right) + \hat{z} \frac{1}{r} \left(\frac{\partial r A_\theta}{\partial r} - \frac{\partial A_r}{\partial \theta} \right). \tag{11}$$

The magnetic flux density vector can be expressed as

$$\begin{Bmatrix} B_r \\ B_\theta \\ B_z \end{Bmatrix} = \begin{Bmatrix} \frac{1}{r} \frac{\partial A_z}{\partial \theta} - \frac{\partial A_\theta}{\partial z} \\ \frac{1}{r} \frac{\partial A_r}{\partial z} - \frac{\partial A_z}{\partial r} \\ \frac{1}{r} \left(\frac{\partial r A_\theta}{\partial r} - \frac{\partial A_r}{\partial \theta} \right) \end{Bmatrix}, \quad \{B\} = [B_A]\{A_e\}, \tag{12}$$

where the derivative of shape function matrix $[B_A]$ is written as

$$B_A = \begin{bmatrix} 0 & \frac{\partial N_1}{\partial z} & \frac{nN_1}{r} & \dots \\ \frac{\partial N_1}{\partial z} & 0 & -\frac{\partial N_1}{\partial r} & \dots \\ \frac{nN_1}{r} & \frac{1}{r} \frac{\partial(rN_1)}{\partial r} & 0 & \dots \end{bmatrix}. \tag{13}$$

3. Evaluation of elemental matrices

The finite element equations for magnetostrictive/piezoelectric laminate cylindrical shell can be written as

$$\begin{aligned} [M_{uu}^e]\{\ddot{u}^e\} + [C_{uu}^e]\{\dot{u}^e\} + [C_{uA}^e]\{\dot{A}^e\} + [K_{uu}^e]\{u^e\} + [K_{u\phi}^e]\{\phi^e\} - [K_{uA}^e]\{A^e\} &= \{F^e\}, \\ [K_{\phi u}^e]\{u^e\} - [K_{\phi\phi}^e]\{\phi^e\} &= \{G^e\}, \quad -[K_{Au}^e]\{u^e\} - [C_{\phi A}^e]\{\dot{A}^e\} + [K_{AA}^e]\{A^e\} = \{M^e\}, \end{aligned} \tag{14}$$

where $\{F^e\}$, $\{G^e\}$, and $\{M^e\}$ correspond to elemental load vectors of applied mechanical force, electric charge, and magnetic current, respectively. Different elemental matrices in (14) for the n -th harmonic are defined as

$$\begin{aligned} [M_{uu}^e] &= P \int_A [N_u]^T [\rho] [N_u] r \, dr \, dz, & [C_{uA}^e] &= P \int_A [B_u]^T [e] [N_A] r \, dr \, dz, \\ [C_{\phi A}^e] &= P \int_A [B_\phi]^T [\epsilon] [N_A] r \, dr \, dz, & [K_{uu}^e] &= P \int_A [B_u]^T [c] [B_u] r \, dr \, dz, \\ [K_{u\phi}^e] &= P \int_A [B_u]^T [e] [B_\phi] r \, dr \, dz, & [K_{uA}^e] &= P \int_A [B_u]^T [d] [B_A] r \, dr \, dz, \\ [K_{\phi\phi}^e] &= P \int_A [B_\phi]^T [\epsilon] [B_\phi] r \, dr \, dz, & [K_{AA}^e] &= P \int_A [B_A]^T [\mu]^{-1} [B_A] r \, dr \, dz, \end{aligned} \tag{15}$$

where $P = 2\pi$ for $n = 0$ and $P = \pi$ for $n > 0$, and n is the circumferential harmonic number. When electric and magnetic loading are absent, (14) can be written in coupled form as

$$\begin{bmatrix} M_{uu} & 0 & 0 \\ 0 & 0 & 0 \\ 0 & 0 & 0 \end{bmatrix} \begin{Bmatrix} \ddot{u} \\ \ddot{\phi} \\ \ddot{A} \end{Bmatrix} + \begin{bmatrix} C_{uu} & 0 & C_{uA} \\ 0 & 0 & -C_{\phi A} \\ 0 & 0 & 0 \end{bmatrix} \begin{Bmatrix} \dot{u} \\ \dot{\phi} \\ \dot{A} \end{Bmatrix} + \begin{bmatrix} K_{uu} & K_{u\phi} & -K_{uA} \\ K_{\phi u} & -K_{\phi\phi} & 0 \\ -K_{Au} & 0 & K_{AA} \end{bmatrix} \begin{Bmatrix} u \\ \phi \\ A \end{Bmatrix} = \begin{Bmatrix} F(t) \\ 0 \\ 0 \end{Bmatrix}. \tag{16}$$

The magnetic field generated due to mechanical loading will generate current density within the electrically conductive magnetostrictive layer. The finite element equation for current density can be written as

$$\{J^e\} = P \int_A [N]^T \left\{ \sigma \left(\frac{\partial u}{\partial t} \times B \right) + J_0 \right\} r \, dr \, dz. \tag{17}$$

The vector of nodal Lorentz force can be written as

$$\{F^e\} = P \int_A [N]^T \{J \times B\} r \, dr \, dz. \tag{18}$$

This Lorentz force will generate an additional force vector in the equation of motion for the mechanical field. Simultaneous solution of (16) and (18) will account for the effect of the electromagnetic force on the dynamic response of the shell structure.

4. Results and discussions

4.1. Validation. Computer code has been developed to study the effect of electromagnetic force on electric and magnetic response of the structure. The dimensions of the cylinder used for the analysis are $L = 4.0$ m, $R_i = 0.5$ m, and the Terfenol-D and PZT-5A layers are 0.005 m each in thickness. A perfect bonding is assumed between layers and potential noise effects are neglected. The system of equations is solved using the Newmark-beta solution technique. The damping is assumed to be proportional and the damping matrix is derived as $[C_{uu}] = \alpha[M_{uu}] + \beta[K_{uu}]$ where α and β are the proportional damping coefficients depending on natural frequencies of the structure. Damping ratios of 1% and 2% are assumed for first and second modes, respectively, and the values of the proportional damping constants α and β are calculated accordingly.

A rectangular wave made up of a fundamental frequency and its combined odd and even harmonics is used as the load cycle. Each load step, the time increment is applied at 10 equal time intervals. The cylinder is subjected to a uniform internal pressure of 1 N/m² with a clamped-free boundary condition. The electric and magnetic potentials are assumed to be zero at the clamped end. The load vectors corresponding to applied electric charge and magnetic current are also assumed to be zero. The absolute values of nodal velocity and magnetic flux density at the end of first load step are used for calculating the load vector for successive iterations. The results presented below are for the first circumferential harmonics of the shell structure ($n = 1$). A node near the clamped end of the shell giving maximum response is chosen for showing the results. The study is carried out for the Terfenol-D/PZT configuration of the laminate.

The commercial finite element package ANSYS 12.0 is used for the validation studies. The material properties of PZT-5A and Terfenol-D used for the analysis are shown in Tables 1 and 2. ANSYS cannot model fully coupled piezomagnetic material behavior and hence the present code is validated neglecting the piezomagnetic coupling. The response for the validation studies is calculated for the axisymmetric

Elastic constants ($\times 10^9$ N/m ²)					Density (kg/m ³)
C_{11}	C_{12}	C_{23}	$C_{22} = C_{33}$	$C_{44} = C_{66}$	ρ
94.23	40.38	40.38	94.23	26.92	9250
Magnetic permeability ($\times 10^{-6}$ Ns ² /C ²)		Piezomagnetic constants (N/Am)			Electric conductivity ($\times 10^{10}$ S/m)
μ_{11}	$\mu_{22} = \mu_{33}$	q_{11}	q_{12}	q_{35}	σ
6.29	6.29	400	-200	167.67	1.67

Table 1. Material properties of Terfenol-D [Olabi and Grunwald 2008] for radial plane of symmetry.

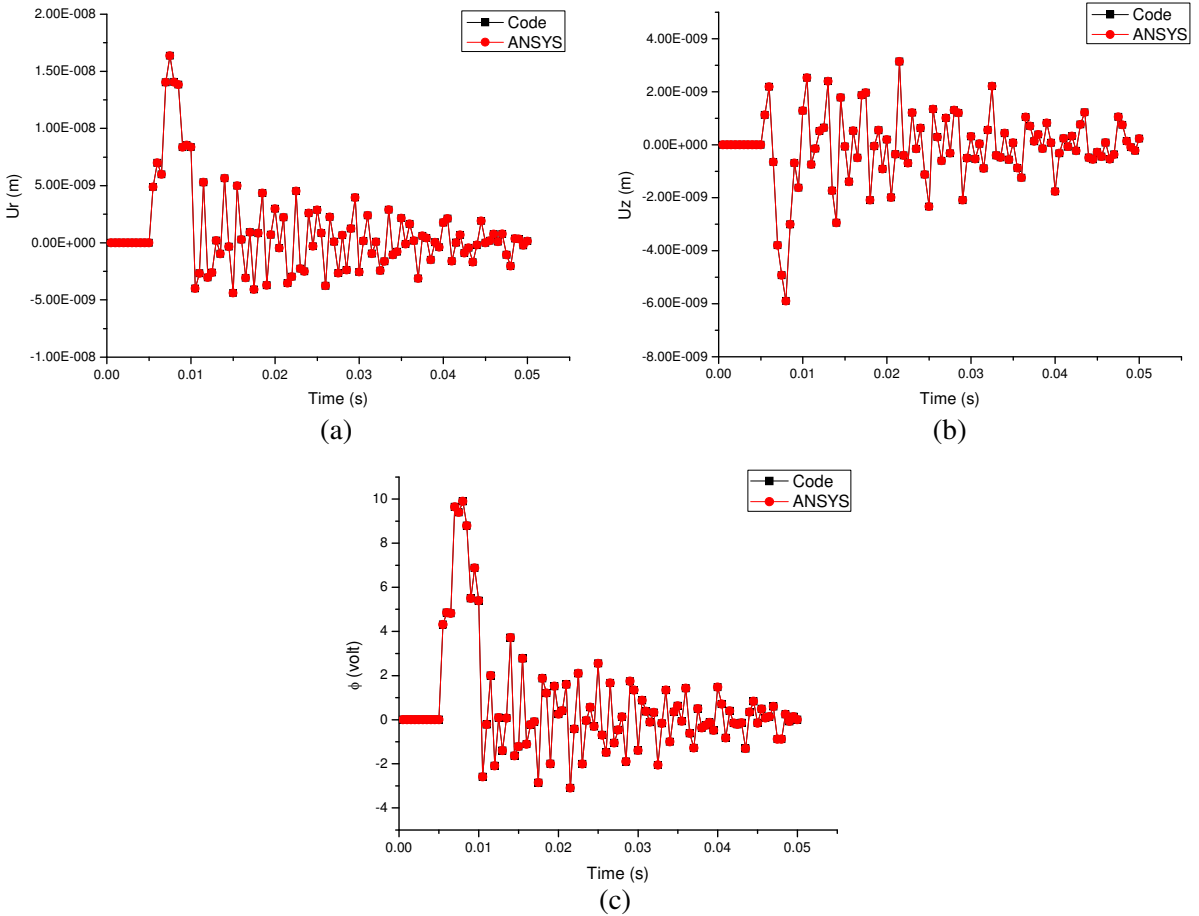


Figure 1. Validation of code for (a) radial displacement u_r , (b) axial displacement u_z , and (c) electric potential ϕ using code and ANSYS.

mode ($n = 0$) of the shell structure. The time harmonic response of the Terfenol-D/PZT laminate shell using our code and ANSYS is shown in Figure 1. It is seen that the result is in good agreement and hence the code is extended to study the dynamic response of fully coupled Terfenol-D/PZT laminate.

Elastic constants ($\times 10^9 \text{ N/m}^2$)					Density (kg/m^3)
C_{11}	C_{12}	C_{23}	$C_{22} = C_{33}$	$C_{44} = C_{66}$	ρ
86.85	54.01	50.77	99.2	21.1	7750
Dielectric constants ($\times 10^{-9} \text{ C/Vm}$)			Piezoelectric constants (C/m^2)		
ϵ_{11}	$\epsilon_{22} = \epsilon_{33}$		e_{11}	e_{12}	e_{35}
1.5	1.53		15.0	-7.2	12.32

Table 2. Material properties of PZT-5A [Chen et al. 2007] for radial plane of symmetry.

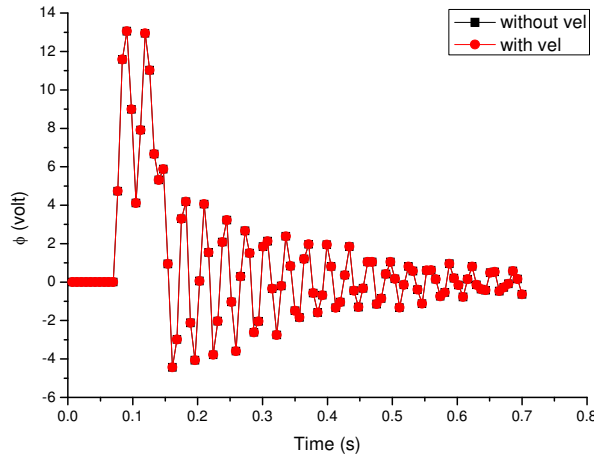


Figure 2. Variation of electric potential ϕ without and with consideration of the velocity effect.

4.2. Dynamic response of clamped-free Terfenol-D/PZT shell. The time harmonic response is calculated without considering the velocity effect and with the velocity effect after the first duty cycle of mechanical loading. Figure 2 represents the variation of electric potential (ϕ) of a node near the clamped end of the shell with and without considering the effect of velocity and the derived electromagnetic force. It is seen that there is no significant variation in the response when the dynamic electromagnetic force is accounted for. This is because the magnetic field generated due to piezomagnetic coupling of Terfenol-D is too small to influence the dynamic response.

Figure 3 shows the variation of the magnetic vector potential in the radial (A_r), circumferential (A_θ), and axial (A_z) directions without and with considering the effect of velocity in the dynamic response. It is seen that the axial component of the magnetic vector potential is the dominant component, so its influence on the electric field will be more in the axial direction.

The magnetic flux density generated in the radial (B_r), circumferential (B_θ), and axial (B_z) directions is shown in Figure 4a. The absolute value of the magnetic flux density in all directions is very small and among the three components, the circumferential component is the significant one. The nodal velocity variation in three directions is shown in Figure 4b.

Numerical studies are carried out by varying the nodal velocities and magnetic vector potentials, in order to understand the influence of velocity on generated electric potential. The nodal velocity and magnetic vector potential are increased independently and as a combination to study the influence of electromagnetic force on dynamic response. Figure 5a shows the variation of electric potential (ϕ) when the nodal velocity is increased from the initial value obtained in a transient analysis. A significant increase in electric potential is noticed when the nodal velocity reaches approximately 3.0 times the initial value. Similarly Figure 5b shows the variation of electric potential (ϕ) when the magnetic vector potential is increased; when the potential reaches 1.74 times the initial value, there is a marked increase. A combination of increase in velocity and magnetic potential is done on a trial and error basis and the variation of electric potential (ϕ) which is relevant in the present study is shown in Figure 5c. It is seen that when the nodal velocity is increased to 2.5 times the initial velocity, a 10% increase in magnetic vector potential will significantly increase the generated electric potential.

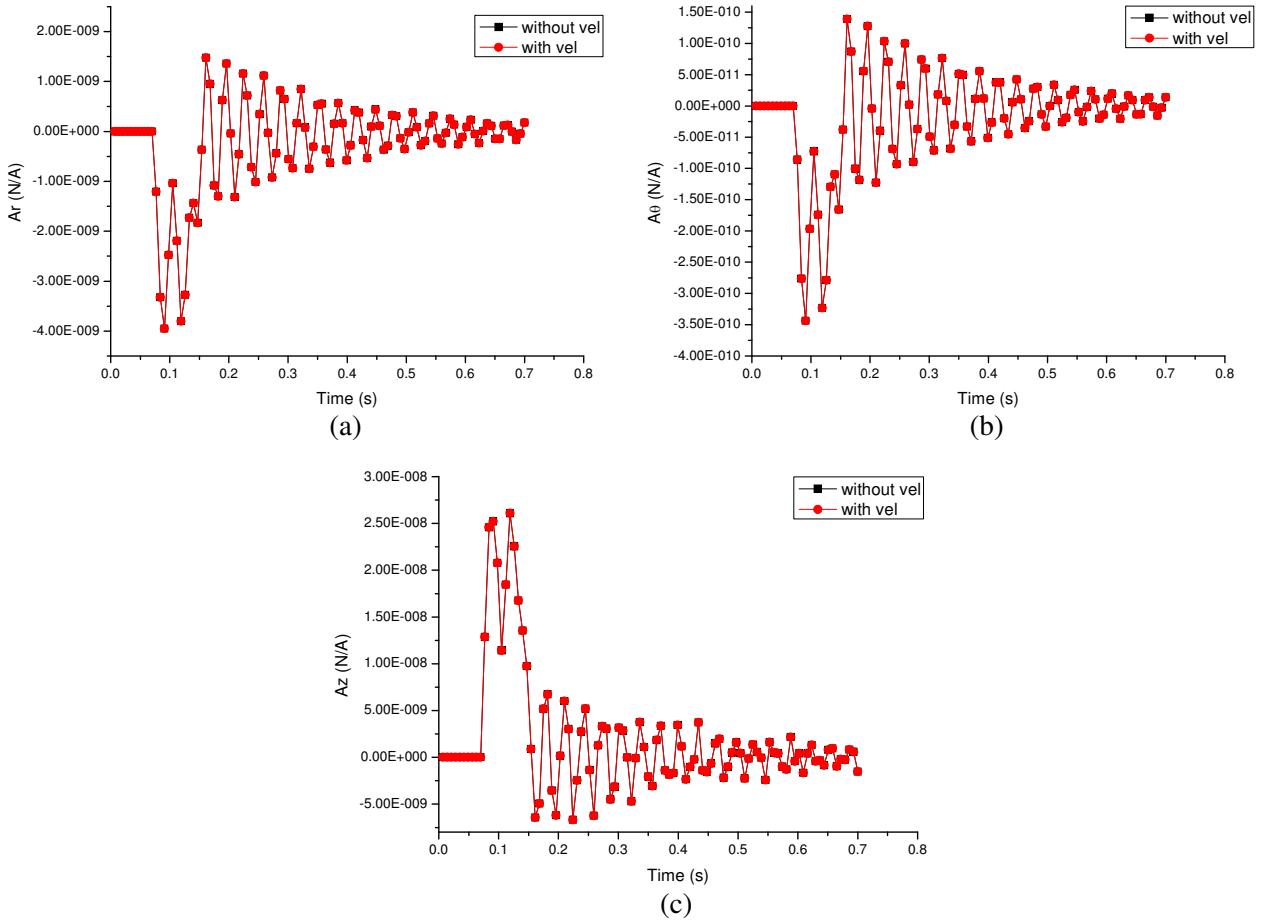


Figure 3. Variation of magnetic vector potential in (a) radial A_r , (b) circumferential A_θ , and (c) axial A_z directions without and with considering velocity effect.

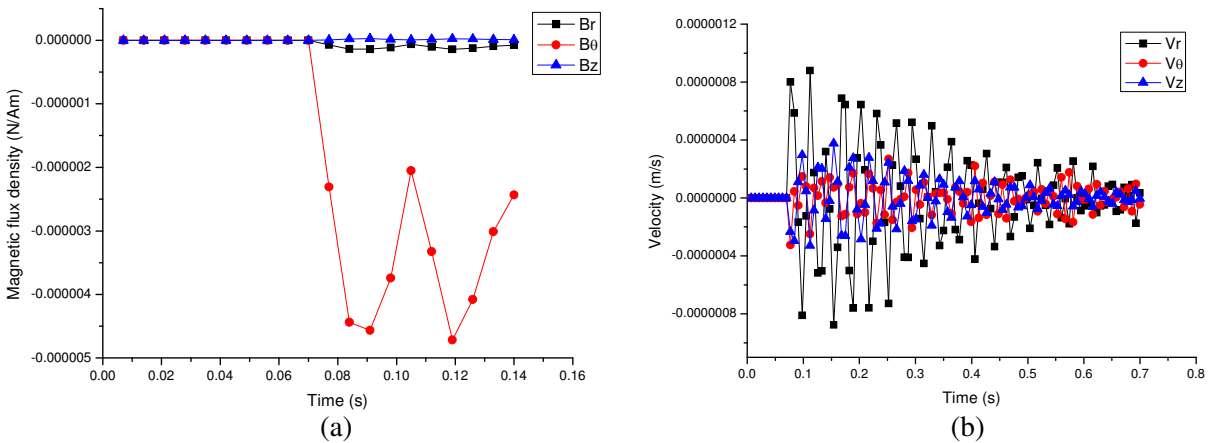


Figure 4. Variation of (a) magnetic flux density and (b) nodal velocity in radial, circumferential, and axial directions.

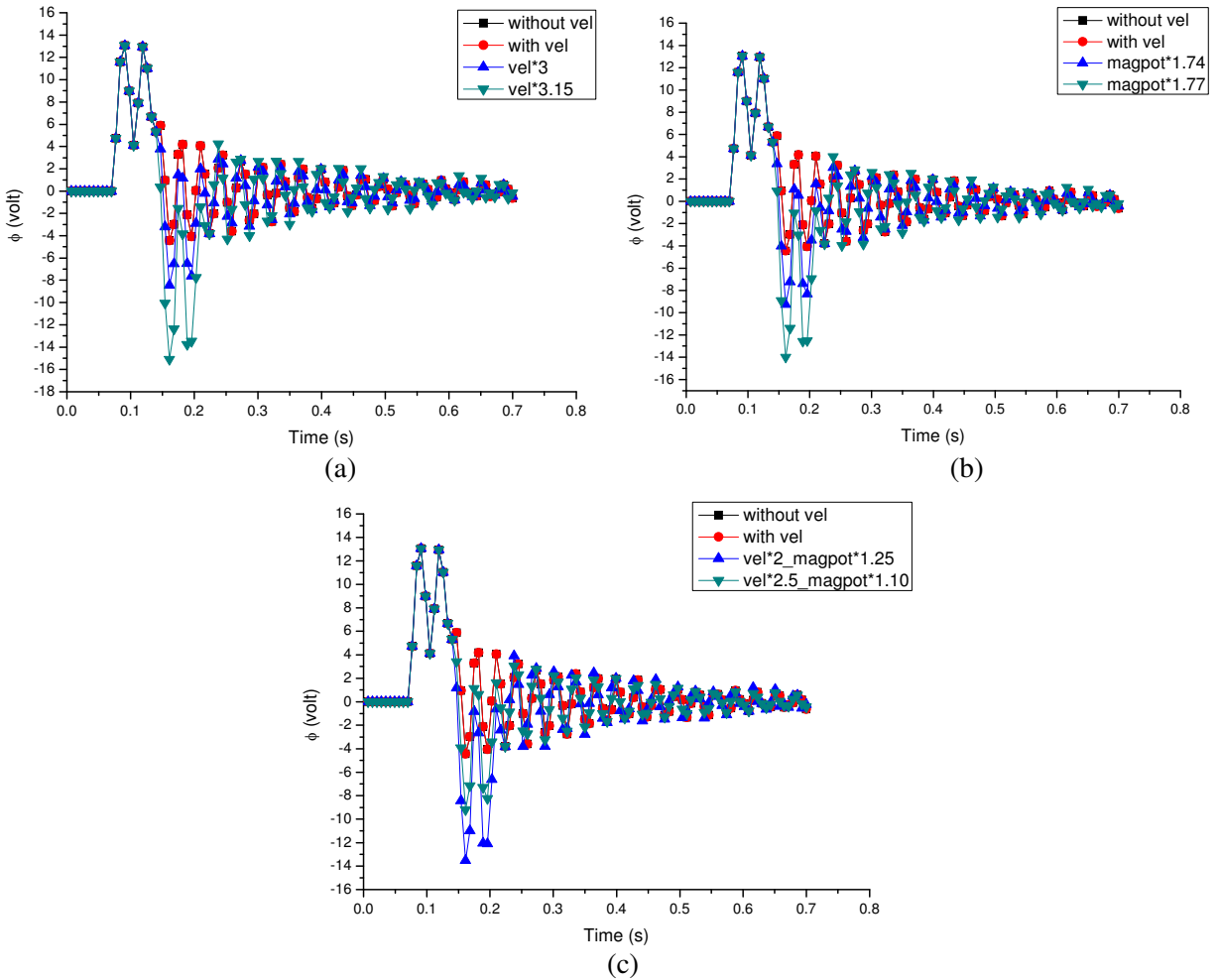


Figure 5. Variation of electric potential ϕ with (a) increased nodal velocity, (b) increased magnetic vector potential, and (c) a combination of both.

5. Conclusions

The dynamic response of magnetostrictive/piezoelectric laminate cylindrical shells subjected to uniform internal pressure is studied using a semianalytical finite element method. The Terfenol-D/PZT configuration of the laminate is analyzed for the first circumferential harmonics of the shell structure with a clamped-free boundary condition. Numerical studies are also carried out by varying the nodal velocities and magnetic vector potentials for understanding the influence of velocity on the generated electric potential. The effect of the electromagnetic Lorentz force on dynamic response is marginal at normal operating conditions, but numerical studies suggest that the magnetoelectric effect is significantly influenced by a small increase in magnetic potential at an increased velocity of the shell.

References

- [Biju et al. 2010] B. Biju, N. Ganesan, and K. Shankar, “Finite element formulation using magnetic vector potential approach: effects of displacement current in magneto-electro-elastic cylindrical shells”, *Smart Mater. Struct.* **19**:1 (2010), 015009.
- [Chen et al. 2007] J. Chen, E. Pan, and H. Chen, “Wave propagation in magneto-electro-elastic multilayered plates”, *Int. J. Solids Struct.* **44**:3–4 (2007), 1073–1085.
- [Dai and Wang 2006] H. L. Dai and X. Wang, “Magneto-thermo-electro-elastic transient response in a piezoelectric hollow cylinder subjected to complex loadings”, *Int. J. Solids Struct.* **43**:18–19 (2006), 5628–5646.
- [Hou and Leung 2004] P.-F. Hou and A. Y. T. Leung, “The transient responses of magneto-electro-elastic hollow cylinders”, *Smart Mater. Struct.* **13**:4 (2004), 762–776.
- [Olabi and Grunwald 2008] A. G. Olabi and A. Grunwald, “Design and application of magnetostrictive materials”, *Mater. Des.* **29**:2 (2008), 469–483.
- [Ryu et al. 2001] J. Ryu, A. V. Carazo, K. Uchino, and H.-E. Kim, “Piezoelectric and magnetoelectric properties of lead zirconate titanate/Ni-ferrite particulate composites”, *J. Electroceram.* **7**:1 (2001), 17–24.
- [Shindo et al. 2010] Y. Shindo, K. Mori, and F. Narita, “Electromagneto-mechanical fields of giant magnetostrictive/piezoelectric laminates”, *Acta Mech.* **212**:3–4 (2010), 253–261.
- [Sunar et al. 2002] M. Sunar, A. Z. Al-Garni, M. H. Ali, and R. Kahraman, “Finite element modeling of thermopiezomagnetic smart structures”, *AIAA J.* **40**:9 (2002), 1846–1851.

Received 29 Aug 2010. Revised 12 Dec 2010. Accepted 24 Dec 2010.

B. BIJU: bbiju@rediffmail.com

Machine Design Section, Department of Mechanical Engineering, Indian Institute of Technology Madras, Chennai 600 036, India

N. GANESAN: nganesan@iitm.ac.in

Machine Design Section, Department of Mechanical Engineering, Indian Institute of Technology Madras, Chennai 600 036, India

K. SHANKAR: skris@iitm.ac.in

Machine Design Section, Department of Mechanical Engineering, Indian Institute of Technology Madras, Chennai 600 036, India

JOURNAL OF MECHANICS OF MATERIALS AND STRUCTURES

jomms.org

Founded by Charles R. Steele and Marie-Louise Steele

EDITORS

CHARLES R. STEELE Stanford University, USA
DAVIDE BIGONI University of Trento, Italy
IWONA JASIUK University of Illinois at Urbana-Champaign, USA
YASUHIRO SHINDO Tohoku University, Japan

EDITORIAL BOARD

H. D. BUI École Polytechnique, France
J. P. CARTER University of Sydney, Australia
R. M. CHRISTENSEN Stanford University, USA
G. M. L. GLADWELL University of Waterloo, Canada
D. H. HODGES Georgia Institute of Technology, USA
J. HUTCHINSON Harvard University, USA
C. HWU National Cheng Kung University, Taiwan
B. L. KARIHALOO University of Wales, UK
Y. Y. KIM Seoul National University, Republic of Korea
Z. MROZ Academy of Science, Poland
D. PAMPLONA Universidade Católica do Rio de Janeiro, Brazil
M. B. RUBIN Technion, Haifa, Israel
A. N. SHUPIKOV Ukrainian Academy of Sciences, Ukraine
T. TARNAI University Budapest, Hungary
F. Y. M. WAN University of California, Irvine, USA
P. WRIGGERS Universität Hannover, Germany
W. YANG Tsinghua University, China
F. ZIEGLER Technische Universität Wien, Austria

PRODUCTION contact@msp.org

SILVIO LEVY Scientific Editor

Cover design: Alex Scorpan

Cover photo: Ev Shafir

See <http://jomms.org> for submission guidelines.

JoMMS (ISSN 1559-3959) is published in 10 issues a year. The subscription price for 2011 is US \$520/year for the electronic version, and \$690/year (+ \$60 shipping outside the US) for print and electronic. Subscriptions, requests for back issues, and changes of address should be sent to Mathematical Sciences Publishers, Department of Mathematics, University of California, Berkeley, CA 94720–3840.

JoMMS peer-review and production is managed by EditFLOW™ from Mathematical Sciences Publishers.

PUBLISHED BY
 **mathematical sciences publishers**
<http://msp.org/>

A NON-PROFIT CORPORATION

Typeset in L^AT_EX

Copyright ©2011 by Mathematical Sciences Publishers

Modelling of acoustodiffusive surface waves in piezoelectric-semiconductor composite structures	J. N. SHARMA, K. K. SHARMA and A. KUMAR	791
Dynamic fracture tests of polymethylmethacrylate using a semicircular bend technique	S. HUANG, S.-N. LUO, B. S. A. TATONE and K. XIA	813
Stress and buckling analyses of laminates with a cutout using a {3, 0}-plate theory	ATILA BARUT, ERDOGAN MADENCI and MICHAEL P. NEMETH	827
Electrothermomechanical behavior of a radially polarized rotating functionally graded piezoelectric cylinder	A.G. ARANI, A. LOGHMAN, A. ABDOLLAHITAHERI and V. ATABAKHSHIAN	869
Large-amplitude dynamic analysis of stiffened plates with free edges	ANIRBAN MITRA, PRASANTA SAHOO and KASHINATH SAHA	883
Dynamic behavior of magnetostrictive/piezoelectric laminate cylindrical shells due to electromagnetic force	B. BIJU, N. GANESAN and K. SHANKAR	915
Geometrically nonlinear thermomechanical response of circular sandwich plates with a compliant core	YEOSHUA FROSTIG and OLE THOMSEN	925